Applied Mathematics and Computation 315 (2017) 453–467

Contents lists available at ScienceDirect

Applied Mathematics and Computation

journal homepage: www.elsevier.com/locate/amc

Modification of TV-ROF denoising model based on Split Bregman iterations

Rosanna Campagna[a], Serena Crisci[b], Salvatore Cuomo[a,*], Livia Marcellino[c], Gerardo Toraldo[a]

[a] Department of Mathematics and Applications "R. Caccioppoli", University of Naples Federico II, Italy
[b] Department of Mathematics and Computer Science, University of Ferrara, Italy
[c] Department of Science and Technology, University of Naples Parthenope, Italy

ARTICLE INFO

Article history:
Available online 16 August 2017

Keywords:
Image denoising
TV-ROF model
Split Bregman algorithm
Magnetic Resonance Imaging

ABSTRACT

Minimizing variational models by means of (un)constrained optimization algorithms is a well-known approach for dealing with the image denoising problem. In this paper, we propose a modification of the widely explored TV-ROF model named H-TV-ROF, in which a penalty term based on higher order derivatives is added. A Split Bregman iterative scheme is used to solve the proposed model and its convergence is proved. The performance of the new algorithm is analized and compared with TV-ROF on a set of numerical experiments.

1. Introduction

Digital images are generally corrupted by artefacts, acquisition processes or noise which require effective reconstruction strategies in order to recover important information. The image reconstruction problem is usually formulated as an inverse problem and, in different forms (denoising, filtering, restoration, segmentation, etc.) it arises in various research areas, such as physics, optics, biomedical imaging. In the last years several numerical strategies have been specifically designed for handling, with very different approaches, image reconstruction problems (see for example [2–4,14,18,19,22,29]). The adoption of high performance computing environments in order to deal with the computationally very demanding real applications has been investigated in several works [12,13,21,24].

Our paper is concerned with the efficient numerical solution of the image denoising problem. In image processing a general regularization model can be formulated as

$$u^* := \arg\min_u |\Psi(u)| + H(u), \tag{1}$$

where $|\cdot|$ is a norm and the convex functions $\Psi(u)$ and $H(u)$ are, respectively, the regularization and the fidelity terms. In practice, u generally denote the column vector $u \in \Re^N$ by lexicographical ordering of a two-dimensional image and $u^* \in \Re^N$ is a vector which represents the sought image. Furthermore when $|\cdot|$ is chosen as the ℓ_1-norm, (1) becomes the classical ℓ_1-regularization problem. A special case of (1) is the Rudin–Osher–Fatemi Total Variation (TV-ROF) [25] minimization approach to image denoising

$$u^* := \arg\min_u \|\nabla u\|_1 + \|u - f\|_2^2, \tag{2}$$

* Corresponding author.
E-mail address: salvatore.cuomo@unina.it (S. Cuomo).

http://dx.doi.org/10.1016/j.amc.2017.08.001
0096-3003/

in which an image u^* is recovered starting form its noisy version f, and where ∇u is the gradient of u. A theoretical analysis of this scheme has been proposed by Chambolle and Lions in [11]. The model (2) deals properly with edges and noise removing in gray-scale images and the TV term discourages the solution from having oscillations. Neverthless, despite these nice features, the overall effectiveness of (2) is limited by two main drawbacks:

- it supplies piecewise constant images: smooth regions in original image are recovered as piecewise smooth regions (*staircasing effect*);
- it suffers from the non-linearity and non-differentiability of the TV term.

In order to overcome these difficulties several strategies have been proposed [4,26]. The most commonly used approach consists in modifying the cost function, by adding a penalty terms $R(u)$ in (2), thus defining the new model

$$u^* := \arg\min_u \|\nabla u\|_1 + \|u - f\|_2^2 + R(u). \tag{3}$$

Generally, the choice of $R(u)$ depends on the kind of "a priori" information available on the problem to be solved. Recent studies confirm the advantages of combining TV filter with higher-order differential operators to avoid the well-known *staircasing effect* induced by TV norm, preserving at the same time the image sharpness (see [27] for details). In this paper, we focus on a modification of TV-ROF denoising functional, the *isotropic* TV denoising version, proposed in [10]. In particular our model is formulated as follows:

$$u^* := \arg\min_u \|\nabla u\|_2 + \frac{\mu}{2}\|u - f\|_2^2 + \|\mathcal{H}(u)\|_1, \tag{4}$$

where μ is a real positive number and $\mathcal{H}$ is the Hessian of the function u. Among the many algorithms which have been proposed to solve the TV-ROF problem and its variants, for the numerical solution of (4) we adopted the Split Bregman Algorithm (SBA), proposed in [17] by Goldstein and Osher, which can be seen as a special case of alternating direction method of multipliers (ADMM) [5]. The SBA has been succesfully used in solving several regularized optimization problems [1,16,28] and it has shown to be especially effective for problems involving TV regularization [15,20,26]. Some numerical experiments are carried-out in order to show the benefits of using the second order penalty term in terms of accuracy for image denoising and, furthermore, some experiments on Magnetic Resonance Imaging (MRI) data are reported. Finally, in the Appendix, starting from [9,23], we present a theorem on the convergence of the Split Bregman iterative scheme applied for solving (4). This result it is obtained by extending the proof of Theorems 3.1 and 3.2 for the TV-ROF case, presented in [8].

The paper is organized as follows. In Section 2 some preliminaries about notations are firstly introduced; then, starting from the TV-ROF, we introduce our modified H-TV-ROF model and the related SBA formulation. In Section 3 a computational scheme for the new algorithm is described. Numerical experiments for denoising of synthetic and real images are shown in Section 4. Conclusions and future aims close the paper. The convergence theorem is reported in the Appendix.

2. The H-TV-ROF model

2.1. Preliminaries

Let

$$\Omega = [a_1, b_1] \times [a_2, b_2], \qquad a_1, a_2, b_1, b_2 \in \Re,$$

be a rectangular domain and assume that the function $u \in C^2(\Omega)$. Given $N > 2$, Ω is covered by the regular grid:

$$\Omega_h = \left\{ (x_i, y_j) : \; x_i = a_1 + ih_x, \quad i = 1, \ldots, N, \quad h_x = \frac{b_1 - a_1}{N}, \right.$$
$$\left. y_j = a_2 + jh_y, \quad j = 1, \ldots, N, \quad h_y = \frac{b_2 - a_2}{N} \right\} \subset \Omega. \tag{5}$$

The u values in the mesh points are denoted as

$$u_{i,j} := u(x_i, y_j), \quad i, j = 1, \ldots, N$$

and, in general for any function $g(x, y)$

$$g_{i,j} := g(x_i, y_j), \quad i, j = 1, \ldots, N.$$

Moreover

$$\nabla_x u(x_i, y_j) := (\nabla_x u)_{i,j}, \quad \nabla_y u(x_i, y_j) := (\nabla_y u)_{i,j}$$

are respectively the horizontal and the vertical derivatives in an interior point (x_i, y_j), and therefore the gradient of u at (x_i, y_j) is

$$(\nabla u)_{i,j} \equiv \begin{pmatrix} (\nabla_x u)_{i,j} \\ (\nabla_y u)_{i,j} \end{pmatrix}.$$

We also define:

$$\nabla^{\mathcal{T}}(u)_{i,j} := (\nabla_x u)_{i,j} + (\nabla_y u)_{i,j}.$$

In the following $(\nabla^2_{xx}u)_{i,j}$, $(\nabla^2_{yy}u)_{i,j}$, $(\nabla^2_{xy}u)_{i,j}$ are the second-order derivatives of u at (x_i, y_j); the Laplacian Δ of u at an interior node (x_i, y_j) of Ω is:

$$(\Delta u)_{i,j} := (\nabla^2_{xx}u)_{i,j} + (\nabla^2_{yy}u)_{i,j},$$

whereas the differential operator for the second order derivatives $\mathcal{D}$ is defined as follows:

$$\mathcal{D} := \begin{pmatrix} \nabla^2_{xx} \\ \nabla^2_{yy} \\ \nabla^2_{xy} \end{pmatrix},$$

Finally, $\mathcal{D}^{\mathcal{T}}$ is defined similarly to $\nabla^{\mathcal{T}}$.

2.2. The H-TV-ROF model and SBA iterations

The main feature of the isotropic model consists in using a pixel-wise Euclidean norm for the TV term. This choice is based on the simplified assumption of regarding a digital image as a 2-dimensional matrix of size $N \times N$. The *isotropic TV denoising* model can be defined as:

$$\hat{u} := \arg\min_u \sum_{i,j} \|(\nabla u)_{i,j}\|_2 + \frac{\mu}{2}\sum_{i,j}(u_{i,j} - f_{i,j})^2. \tag{6}$$

Following the idea of the Split Bregman method, (6) can be formulated in terms of the equivalent constrained minimization problem:

$$\hat{u} := \arg\min_u \sum_{i,j} \|d_{i,j}\|_2 + \frac{\mu}{2}\sum_{i,j}(u_{i,j} - f_{i,j})^2, \tag{7}$$

$$\text{s.t.} \quad d = \nabla u.$$

By penalizing the constraint violation, the following unconstrained problem can be defined:

$$\hat{u} := \arg\min_{u,d} \sum_{i,j} \|d_{i,j}\|_2 + \frac{\mu}{2}\sum_{i,j}(u_{i,j} - f_{i,j})^2 + \frac{\lambda}{2}\sum_{i,j}\|d_{i,j} - \nabla u_{i,j}\|_2^2, \tag{8}$$

where $\lambda > 0$ is a fixed penalty parameter. By following [17] the Split Bregman Algoritm (SBA) k-th iteration is defined as follows:

$$u^{k+1} := \arg\min_u \frac{\mu}{2}\sum_{i,j}(u_{i,j} - f_{i,j})^2 + \frac{\lambda}{2}\sum_{i,j}\|d^k_{i,j} - \nabla u_{i,j} - b^k_{i,j}\|_2^2, \tag{9}$$

$$d^{k+1} := \arg\min_d \sum_{i,j} \|d_{i,j}\|_2 + \frac{\lambda}{2}\sum_{i,j}\|d_{i,j} - \nabla u^{k+1}_{i,j} - b^k_{i,j}\|_2^2, \tag{10}$$

$$b^{k+1} := b^k_{i,j} + (\nabla u^{k+1}_{i,j} - d^{k+1}_{i,j}), \tag{11}$$

where b^0 is set equal to 0.

In our model we add a second-order regularization term to the isotropic model (6) which becomes:

$$\hat{u} := \arg\min_u \sum_{i,j} \|(\nabla u)_{i,j}\|_2 + \frac{\mu}{2}\sum_{i,j}(u_{i,j} - f_{i,j})^2 + \beta\sum_{i,j}\|\mathcal{H}(u_{i,j})\|_1,$$

where $\mathcal{H}$ denotes the Hessian. The ℓ_1–norm of $\mathcal{H}(u_{i,j})$ can be approximated by the *LogSumExp (LSE) function* [6] which is the convex and infinitely differentiable function defined as:

$$LSE(x_1, \ldots, x_n) := \log(\exp(x_1) + \cdots + \exp(x_n)).$$

Therefore, our model, with a second order penalty term, becomes:

$$\begin{aligned}\hat{u} : = \arg\min_u &\sum_{i,j} \|(\nabla u)_{i,j}\|_2 + \frac{\mu}{2}\sum_{i,j}(u_{i,j} - f_{i,j})^2 \\ &+ \beta\sum_{i,j}\log(\exp(\nabla^2_{xx}u + \nabla^2_{xy}u)_{i,j} + \exp(\nabla^2_{yy}u + \nabla^2_{xy}u)_{i,j}).\end{aligned} \tag{12}$$

In the sequel we will refer to (12) as H-TV-ROF model, where H stands for Hessian. Let now define the auxiliary variables $d \equiv (d_x, d_y)^T$, $h \equiv (h_{xx}, h_{yy}, h_{xy})^T$, and let consider the constrained problem

$$\begin{aligned} \hat{u} : = & \arg\min_{u} \sum_{i,j} \|d_{i,j}\|_2 + \frac{\mu}{2} \sum_{i,j} (u_{i,j} - f_{i,j})^2 \\ & + \beta \sum_{i,j} \log(\exp(h_{xx} + h_{xy})_{i,j} + \exp(h_{yy} + h_{xy})_{i,j}) \\ & \text{s.t.} \quad d = \nabla u \quad \text{and} \quad h = \mathcal{D}u, \end{aligned} \tag{13}$$

thus, by penalizing the constraints violation, we end up with the unconstrained minimization problem

$$\begin{aligned} \hat{u} : = & \arg\min_{u,d,h} \sum_{i,j} \|d_{i,j}\|_2 + \frac{\mu}{2} \sum_{i,j} (u_{i,j} - f_{i,j})^2 + \frac{\lambda}{2} \sum_{i,j} \|d_{i,j} - \nabla u_{i,j}\|_2^2 \\ & + \frac{\lambda}{2} \sum_{i,j} \|h_{i,j} - \mathcal{D}u_{i,j}\|_2^2. \end{aligned} \tag{14}$$

Similarly as for the TV-ROF problem (7), for the H-TV-ROF Problem, the following SBA formulation can be defined:

$$\begin{aligned} u^{k+1} : = & \arg\min_{u} \sum_{i,j} \frac{\mu}{2} (u_{i,j} - f_{i,j})^2 + \frac{\lambda}{2} \sum_{i,j} \|d_{i,j}^k - \nabla u_{i,j} - b_{i,j}^k\|_2^2 \\ & + \frac{\lambda}{2} \sum_{i,j} \|h_{i,j}^k - \mathcal{D}u_{i,j} - c_{i,j}^k\|_2^2, \end{aligned} \tag{15}$$

$$d^{k+1} := \arg\min_{d} \sum_{i,j} \|d_{i,j}\|_2 + \frac{\lambda}{2} \sum_{i,j} \|d_{i,j} - \nabla u_{i,j}^{k+1} - b_{i,j}^k\|_2^2, \tag{16}$$

$$\begin{aligned} h^{k+1} : = & \arg\min_{h} \beta \sum_{i,j} \log\big(\exp(h_{xx} + h_{xy})_{i,j}) + \exp(h_{yy} + h_{xy})_{i,j}\big) \\ & + \frac{\lambda}{2} \sum_{i,j} \|h_{i,j} - \mathcal{D}u_{i,j}^{k+1} - c_{i,j}^k\|_2^2, \end{aligned} \tag{17}$$

$$b^{k+1} := b_{i,j}^k + (\nabla u_{i,j}^{k+1} - d_{i,j}^{k+1}), \tag{18}$$

$$c^{k+1} := c_{i,j}^k + (\mathcal{D}u_{i,j}^{k+1} - h_{i,j}^{k+1}), \tag{19}$$

where λ, $\mu > 0$ are fixed penalty parameters and the auxiliary variables b^0 and c^0 are set equal to 0. We recall that for any convex function F: $\Re^n \to \Re$ the *subdifferential* of F in u is defined as

$$\partial F(u) = \{p \in \Re^n : F(v) \geq F(u) + \langle p, v - u \rangle, \forall v \in domF\},$$

where $\langle \cdot, \cdot \rangle$ is the scalar product, $domF$ is the domain of the function F and every element $p \in \partial F$ is a *subgradient* of F in u.

The Euler-Lagrange conditions for (15–17) are respectively:

$$\mu(u_{i,j}^{k+1} - f_{i,j}) - \lambda \nabla^T (d_{i,j}^k - \nabla u_{i,j}^{k+1} - b_{i,j}^k) + \lambda \mathcal{D}^T (h_{i,j}^k - \mathcal{D}u_{i,j}^{k+1} - c_{i,j}^k) = 0, \tag{20}$$

$$p_{i,j}^{k+1} + \lambda (d^{k+1_{i,j}} - \nabla u_{i,j}^{k+1} - b_{i,j}^k) = 0, \tag{21}$$

$$\beta \nabla J(h_{i,j}^{k+1}) + \lambda (h_{i,j}^{k+1} - \mathcal{D}u_{i,j}^{k+1} - c_{i,j}^k) = 0, \tag{22}$$

where $p_{i,j}^{k+1} \in \partial \|d_{i,j}^{k+1}\|_2$ and $J(h) = \log\big(\exp(h_{xx} + h_{xy})) + \exp(h_{yy} + h_{xy})\big)$, with $h \equiv (h_{xx}, h_{yy}, h_{xy})$. It is possible to show that, under suitable hypothesis on the second order derivatives,

$$\lim_{k \to \infty} u^k = \hat{u},$$

wehere $\{u_k\}$ is the sequence generated by the Split Bregman iterative scheme (15–19) and $\hat{u}$ is solution of H-TV-ROF problem. A proof of this result is given in the Appendix to this paper, similar to the one proposed by Cai et al. in [8] for the convergence of the inexact Split Bregman scheme for a general unconstrained minimization problem.

3. The computational scheme

An algorithmic framework for solving (15–17) can be formulated starting from the optimality conditions (20–22). In particular, collecting terms in (20) we obtain the equation

$$(-\mu - \lambda\Delta + \lambda\mathcal{D}^{\mathcal{T}}\mathcal{D})u_{i,j}^{k+1} = -\mu f_{i,j} - \lambda\nabla^{\mathcal{T}}(d_{i,j}^{k} - b_{i,j}^{k}) + \lambda\mathcal{D}^{\mathcal{T}}(h_{i,j}^{k} - c_{i,j}^{k}) \tag{23}$$

from which is formally possible to compute u^{k+1}. About d^{k+1}, from Eq. (20) we have

$$0 = \frac{d_{i,j}^{k+1}}{\|d_{i,j}^{k}\|_2} + \lambda(d_{i,j}^{k+1} - \nabla u_{i,j}^{k} - b_{i,j}^{k}).$$

We now proceed similarly as in [17]; by approximating $\|d_{i,j}^{k}\|_2$ with $s_{i,j}^{k}$, where $s_{i,j}^{k} = \|\nabla u_{i,j}^{k} + b_{i,j}^{k}\|_2$ we obtain:

$$d_{i,j}^{k+1} = \frac{s_{i,j}^{k}\lambda(\nabla u_{i,j}^{k} + b_{i,j}^{k})}{s_{i,j}^{k}\lambda + 1}. \tag{24}$$

Finally, about h, a component-wise formulation can be derived by the optimality condition (22). Let $c = (c_{xx}, c_{yy}, c_{xy})$ defined as in (19), by solving with respect to $(h_{xx})_{i,j}$ (the same can obviously be done by solving with respect to $(h_{yy})_{i,j}$) we get

$$0 = \beta\frac{\exp((h_{xx}^{k+1}))_{i,j}}{\exp(h_{xx}^{k})_{i,j} + \exp(h_{yy}^{k})_{i,j}} + \lambda((h_{xx}^{k+1})_{i,j} - \nabla_{xx}^{2}u_{i,j}^{k+1} - (c_{xx}^{k})_{i,j}).$$

If we approximate the exponential function with the first-order Taylor expansion:

$$\frac{\exp(h_{xx}^{k+1})_{i,j}}{\exp(h_{xx}^{k})_{i,j} + \exp(h_{yy}^{k})_{i,j}} \approx \frac{1 + (h_{xx}^{k+1})_{i,j}}{2 + (h_{xx}^{k})_{i,j} + (h_{yy}^{k})_{i,j}},$$

and we define

$$t_{i,j}^{k} := 2 + (h_{xx}^{k})_{i,j} + (h_{yy}^{k})_{i,j},$$

we eventually obtain

$$(h_{xx}^{k+1})_{i,j} = \frac{\lambda t_{i,j}^{k}}{\lambda t_{i,j}^{k} + \beta}(\nabla_{xx}^{2}u_{i,j}^{k+1} + (c_{xx}^{k})_{i,j}) - \frac{\beta}{\lambda t_{i,j}^{k} + \beta}, \tag{25a}$$

$$(h_{yy}^{k+1})_{i,j} = \frac{\lambda t_{i,j}^{k}}{\lambda t_{i,j}^{k} + \beta}(\nabla_{yy}^{2}u_{i,j}^{k+1} + (c_{yy}^{k})_{i,j}) - \frac{\beta}{\lambda t_{i,j}^{k} + \beta}, \tag{25b}$$

$$(h_{xy}^{k+1})_{i,j} = \nabla_{xy}^{2}u_{i,j}^{k+1} + (c_{xy}^{k})_{i,j} - \frac{\beta}{\lambda}, \tag{25c}$$

where the equation (25c) is obtained by solving the equation

$$0 = \beta + \lambda((h_{xy}^{k+1})_{i,j} - \nabla_{xy}^{2}u_{i,j}^{k+1} - (c_{xy}^{k})_{i,j}),$$

with respect to h_{xy}^{k+1}. Hence, our computational scheme can be summarized as follows:

Modified Split Bregman Isotropic TV Denoising
Inizialize: $u^0 = f, d^0 = b^0 = c^0 = h^0 = 0$
While: $\|u^{k+1} - u^k\|_2 > tol$
Compute u^{k+1} by (23)
Compute d^{k+1} by (24)
Compute h^{k+1} by (25a–25c)
End

The numerical solutions are computed using a finite-difference (FD) scheme for approximating all the partial derivatives and differential operators. Specifically, we have adopted a centered finite-difference scheme at interior points and one-sided (backward or forward) finite-difference at the boundaries of the image. For our problems we adopted Dirichlet boundary conditions (i.e. the values of the function at the boundaries are specified). The FD scheme applied to (25a–25c) generates a system of equations that can be solved in different ways, according to the intrinsic properties of the problem: as suggested in [17] we use one sweep of the Gauss-Seidel method.

Table 1
Values corresponding to restored images in Fig. 1.

Denoising algorithm	Image	PSNR (dB)	Relative error
TV-ROF	Cameraman	24.5156	0.011704
	Spiral	24.3347	0.015036
	Lena	24.3268	0.015491
H-TV-ROF	Cameraman	25.6337	0.012705
	Spiral	27.4950	0.012064
	Lena	26.4955	0.013536

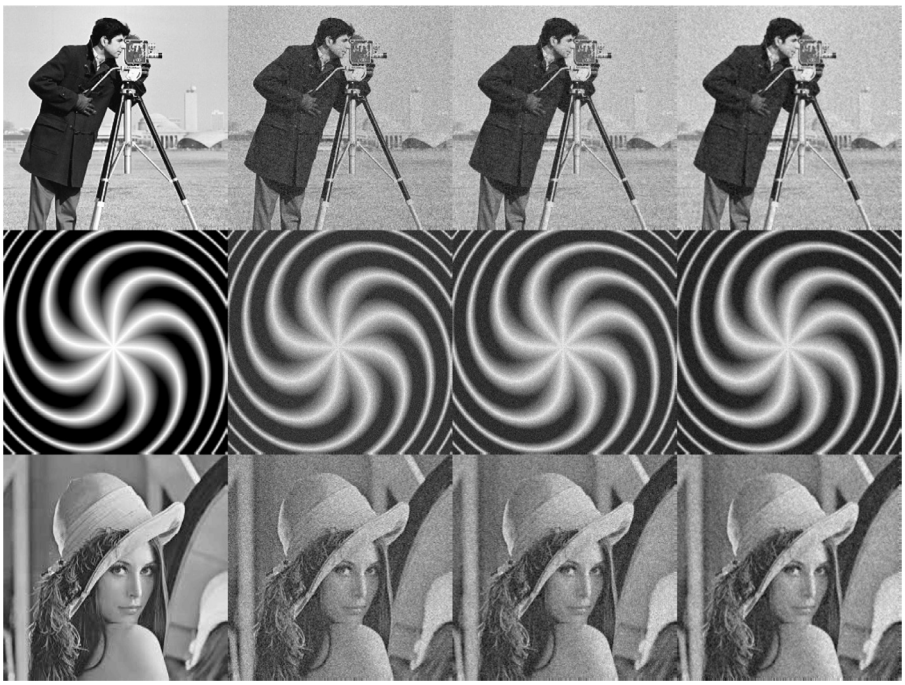

Fig. 1. From left to right the frames show, respectively, the original image, the noisy image (Gaussian noise), the restored TV-ROF image, the restored H-TV-ROF image.

4. Numerical experiments

In this section we report numerical results that compare H-TV-ROF and TV-ROF on the image denoising problem using a set of standard grayscale and MRI images. The implementation has been done in Matlab R2016b. We adopted the *Peak Signal-to-Noise Ratio* (PSNR) to evaluate the quality of output images, defined as follows:

$$PSNR = 10 \cdot \log_{10} \frac{\max(X)}{\mathrm{mse}(X, u)},$$

where $\max(X)$ is the maximum intensity value of the original image X and $\mathrm{mse}(X, u)$ is the mean square error between X and the denoised image u. As usual, the PSNR is expressed in terms of the logarithmic decibel scale. For each case study, we have performed a set of numerical tests with the values of the parameters λ, μ and β chosen on the basis of our computational experiments.

4.1. Case study 1: grayscale images

We start by examining the problem of image denoising using three standard grayscale images (*Cameraman*, *Spiral*, *Lena*). The original images are corrupted with 2% of Gaussian noise. Table 1 illustrates the performance of the two algorithms, with the setting of $\mu = 1.5,\ \lambda = 0.05,\ \beta = 1.9$ for the parameters. The higher values of PSNR show that the second order derivatives term leads to better restored images. This is visually confirmed by Fig. 1. Moreover, in *Spiral* and *Lena* images we can observe a decrease of relative errors.

Table 2
Quality test on a 2D Shepp–Logan phantom image.

Denoising algorithm	Noise (%)	PSNR (dB)	Iteration
	3	29.37	10
TV-ROF	5	25.75	11
	9	21.07	13
	3	28.88	8
H-TV-ROF	5	26.27	9
	9	22.20	10

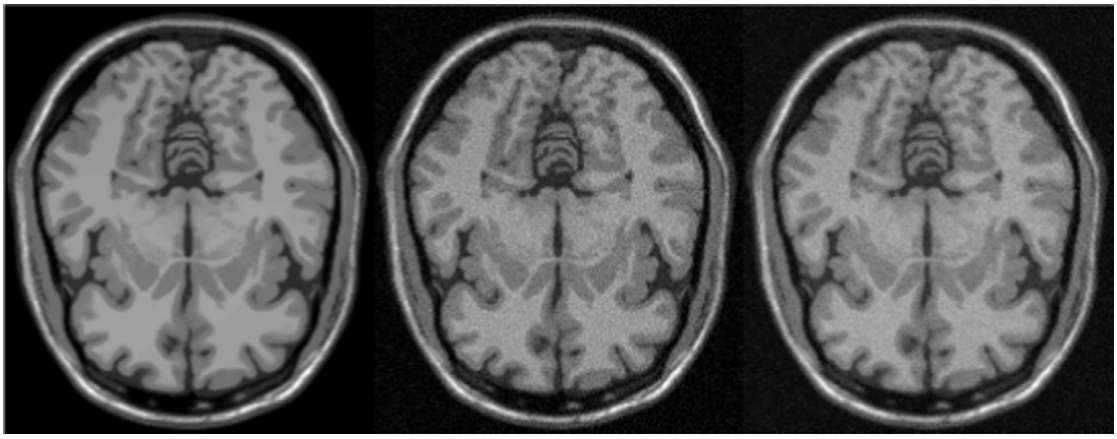

Fig. 2. From left to right: Ground Truth, noisy image with $PS = T1,\ NL = 5\%$; restored image.

Table 3
Quality test on a T1 brain web dataset.

Denoising algorithm	Noise (%)	PSNR (dB)	Iteration
	1	44.11	2
TV-ROF	3	34.58	2
	5	30.09	2
	1	40.53	3
H-TV-ROF	3	34.7	2
	5	34.59	2

4.2. Case study 2: MRI denoising of brain images

Our algorithm has been tested on a 2D Shepp–Logan phantom, by applying three different percentages of Gaussian noise. Table 2 reports the values obtained for $\mu = 1.9,\ \lambda = 0.05,\ \beta = 0.4$. Afterwards we have considered a simulated 3D brain MRI image dataset produced by a MRI simulator.[1] This 3D simulator gives 181 images, each of size 217×181, that are generated by varying specific imaging parameters and artifacts. Then we have analyzed several images (slices of the 3D dataset) with three different pulse sequences ($PS = \{T1, T2, PD\}$) and noise levels. The noise level percentage (relative to the brightest tissue)(NL) has been set equal to 1%, 3%, 5%, 7%, 9%. For a global analysis, the visual inspection of the denoised images is presented, specifically for regions containing some relevant structure (i.e. central slices) shown in Fig. 2. As in the previous case study, in order to estimate the performance of H-TV-ROF, we have considered the PSNR and the relative error estimate. For T1 pulse sequence we set $\mu = 1.9,\ \lambda = 0.06,\ \beta = 0.005$, while for T2 and Proton density pulse sequences we have assigned $\mu = 1.9,\ \lambda = 0.04,\ \beta = 0.005$. As expected the quality of the denoised image deteriorates when the noise increase, as shown in Tables 2–4. Such deterioration is mitigated with the H-TV-ROF model as shown Tables 2 and 3. This is especially evident for the T1 image denoising with 5% of noise level.

4.3. Case study 3: MRI denoising of real images of a knee

Finally, we have tested H-TV-ROF on slices of a real 3D knee MRI dataset. In particular, we have performed two different case studies: i) a low resolution images denoising; ii) the reconstruction of a high resolution MRI image, assumed as *Ground Truth*, that has been corrupted by 5% noise level.

[1] Brainweb dataset: http://brainweb.bic.mni.mcgill.ca/

Table 4
Quality test on a single central slice of a simulated 3D brain MRI image with increasing noise.

Pulse sequence	Noise (%)	PSNR	Rel. error	Iterations	Execution time (s)
	1	40.5296	0.007288	3	0.38791
T1	3	34.7034	0.024236	2	0.352572
	5	30.6141	0.042607	3	0.483256
	1	35.1379	0.013182	3	0.478549
T2	3	30.0766	0.038759	4	0.397612
	5	26.3093	0.067752	3	0.327295
	1	37.2733	0.005555	2	0.341341
Proton density	3	30.9288	0.020124	2	0.354039
	5	26.7636	0.035474	2	0.239194

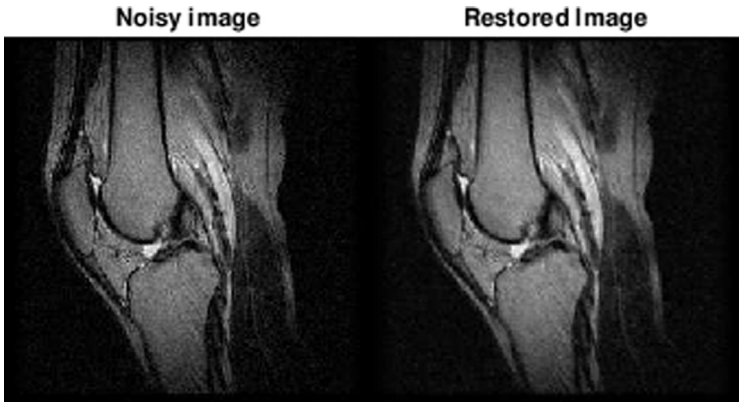

Fig. 3. A central slice of a real knee MRI image. From left to right the frames show: the original low resolution image and the restored image.

Table 5
Relative error estimation and execution times.

Rel. error estim.	Execution time (s)
0.734×10^{-3}	0.675473
0.867×10^{-3}	0.532719
0.743×10^{-3}	0.571054
0.749×10^{-3}	0.570331
0.649×10^{-3}	0.657509

Fig. 3 clearly shows an improvement of the image quality. Furthermore, Table 5 reports the relative error estimation and execution times for different slices, with $\mu = 1.9,\ \lambda = 0.05,\ \beta = 0.005$. The quality of the restored image is confirmed by the values of the PSNR equal to 28.6761 dB in 9 iterations and the relative error of magnitude 0.0816134 in the elapsed time of 3.065753 s. The visual inspection confirms the quality of the denoised image (see Fig. 4). Finally, the performances of the model have been investigated also by comparing the gray level profiles of the input image with the denoised one (see Fig. 5).

5. Conclusions and future aims

In this paper we have proposed a novel denoising model based on a penalty term with second order derivatives. Moreover, the convergence of the adapted Split Bregman iterative scheme to solve this problem has been proved. Numerical experiments confirm the advantages of the proposed scheme to avoid the staircasing effect induced by TV norm and we also observe the ability of our algorithm to improve the contrast and to lift image visual quality. This last feature is very useful in real image denoising of MRI data. Finally, we observe that the choice of such parameters in the models, as for example how to optimally weigh the penalty term, is a general and open question. To address this issue several of methodologies are known and therefore one of our future aims is to investigate on the impact of the parameter values on the proposed models.

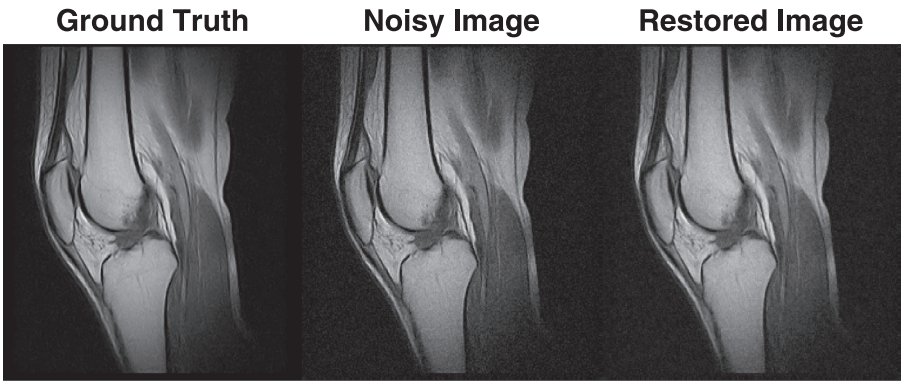

Fig. 4. A central slice of a real knee MRI image. From left to right the frames show: the original high resolution image, the noisy image (5% Gaussian noise) and the restored image.

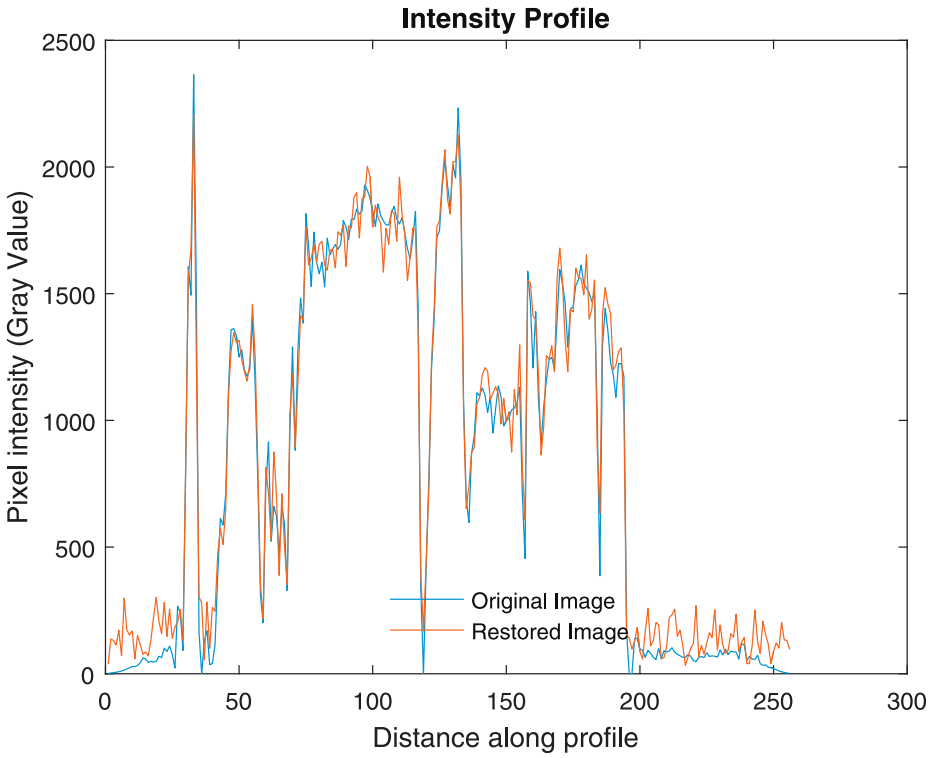

Fig. 5. The behavior of the restored image follows the one of the original image (Fig. 3); the gap between the profiles is due to the noise level introduced.

Appendix

We, first, recall two properties of the norm, which will be useful for proving Theorem 1. Let H be an Hilbert space. For any $x, y \in H$ we have:

1. $\|x+y\|^2 = \|x\|^2 + \|y\|^2 + 2\langle x, y\rangle$,
2. $\|x+y\|^2 + \|x-y\|^2 = 2\|x\|^2 + 2\|y\|^2$ *(parallelogram law).*

Let $u \in C^4(\Omega)$, and $f \in L^2(\Omega)$ and let consider the problem

$$\min_u \|\nabla u\|_2 + \frac{\mu}{2}(u-f)^2 + \beta \log\left(\exp(\nabla^2_{xx}u + \nabla^2_{xy}u) + \exp(\nabla^2_{yy}u + \nabla^2_{xy}u)\right) \tag{26}$$

The SBA formulation for problem (26) is:

$$\begin{aligned} u^{k+1} = \arg\min_u \frac{\mu}{2}\|u-f\|_2^2 &+ \frac{\lambda}{2}\|d_x^k - \nabla_x u - b_x^k\|_2^2 + \frac{\lambda}{2}\|d_y^k - \nabla_y u - b_y^k\|_2^2 \\ &+ \frac{\lambda}{2}\|h_{xx}^k - \nabla_x^2 u - c_{xx}^k\|_2^2 + \frac{\lambda}{2}\|h_{yy}^k - \nabla_y^2 u - c_{yy}^k\|_2^2 \\ &+ \frac{\lambda}{2}\|h_{xy}^k - \nabla_y\nabla_x u - c_{xy}^k\|_2^2, \end{aligned} \tag{27}$$

$$\begin{aligned} (d_x^{k+1}, d_y^{k+1}) = \arg\min_{d_x,d_y} \|(d_x,d_y)\|_2 + + \frac{\lambda}{2}\|d_x - \nabla_x u^{k+1} - b_x^k\|_2^2 \\ + \frac{\lambda}{2}\|d_y - \nabla_y u^{k+1} - b_y^k\|_2^2, \end{aligned} \tag{28}$$

$$\begin{aligned} (h_{xx}^{k+1}, h_{yy}^{k+1}, h_{xy}^{k+1}) = \arg\min_{h_{xx},h_{yy},h_{xy}} &\beta\log\big(\exp(d_{xx}+d_{xy}) + \exp(d_{yy}+d_{xy})\big) \\ &+ \frac{\lambda}{2}\|h_{xx} - \nabla_x^2 u^{k+1} - c_{xx}^k\|_2^2 + \frac{\lambda}{2}\|h_{yy} - \nabla_y^2 u^{k+1} - c_{yy}^k\|_2^2 \\ &+ \frac{\lambda}{2}\|h_{xy} - \nabla_y\nabla_x u^{k+1} - c_{xy}^k\|_2^2, \end{aligned} \tag{29}$$

$$\begin{aligned} b_x^{k+1} &= b_x^k + (\nabla_x u^{k+1} - d_x^{k+1}), \\ b_y^{k+1} &= b_y^k + (\nabla_y u^{k+1} - d_y^{k+1}), \\ c_{xx}^{k+1} &= c_{xx}^k + (\nabla_x^2 u^{k+1} - h_{xx}^{k+1}), \\ c_{yy}^{k+1} &= c_{yy}^k + (\nabla_y^2 u^{k+1} - h_{yy}^{k+1}), \\ c_{xy}^{k+1} &= c_{xy}^k + (\nabla_y\nabla_x u^{k+1} - h_{xy}^{k+1}). \end{aligned} \tag{30}$$

Theorem 1. *Let be $\lambda \in \mathbb{R}^+$. Assume that there exist a solution u^* of H-TV-ROF problem (26) and $\delta_1, \delta_2, \delta_3 \in (0,1)$ such that, for each $k \in \mathbb{N}$, $\|\nabla_x^2 u_e^k\| \le \delta_1$, $\|\nabla_y^2 u_e^k\| \le \delta_2$, $\|\nabla_y\nabla_x u_e^k\| \le \delta_3$, where u^k is defined in (27) and $u_e^k = u^k - u^*$. Then*

$$\lim_{k\to\infty}\|u^k - u^*\| = 0. \tag{31}$$

Proof. Let u^* be an arbitrary solution of (26).

Let

$$b_x^* = \frac{1}{\lambda}p_x^* := \frac{1}{\lambda}\frac{|d_x^*|}{\|(d_x^*,d_y^*)\|_2}, \quad b_y^* = \frac{1}{\lambda}p_x^* := \frac{1}{\lambda}\frac{|d_y^*|}{\|(d_x^*,d_y^*)\|_2}, \quad c_{xy}^* = \beta,$$

$$c_{xx}^* = \frac{1}{\beta}q_{xx}^* := \frac{1}{\beta}\frac{\exp(d_{xx}^*)}{\exp(d_{xx}^*)+\exp(d_{yy}^*)}, \quad c_{yy}^* = \frac{1}{\beta}q_{yy}^* := \frac{1}{\beta}\frac{\exp(d_{yy}^*)}{\exp(d_{xx}^*)+\exp(d_{yy}^*)}.$$

Then it holds:

$$\begin{aligned} 0 = \mu(u^*-f) &- \lambda\nabla_x(d_x^* - \nabla_x u^* - b_x^*) - \lambda\nabla_y(d_y^* - \nabla_y u^* - b_y^*) \\ &+ \lambda\nabla_x^2(h_{xx}^* - \nabla_x^2 u^* - c_{xx}^*) + \lambda\nabla_y^2(h_{yy}^* - \nabla_y^2 u^* - c_{yy}^*) \\ &+ \lambda\nabla_{xy}(h_{xy}^* - \nabla_{xy}u^* - c_{xy}^*), \end{aligned} \tag{32}$$

$$\begin{aligned} 0 &= p_x^* + \lambda(d_x^* - \nabla_x u^* - b_x^*), \\ 0 &= p_y^* + \lambda(d_y^* - \nabla_y u^* - b_y^*), \\ 0 &= \beta q_{xx}^* + \lambda(h_{xx}^* - \nabla_x^2 u^* - c_{xx}^*), \\ 0 &= \beta q_{yy}^* + \lambda(h_{yy}^* - \nabla_y^2 u^* - c_{yy}^*), \\ 0 &= \beta + \lambda(h_{xy}^* - \nabla_{xy}u^* - b_{xy}^*), \end{aligned} \tag{33}$$

$$\begin{aligned} b_x^* &= b_x^* + (\nabla_x u^* - d_x^*), \\ b_y^* &= b_y^* + (\nabla_y u^* - d_y^*), \\ c_{xx}^* &= c_{xx}^* + (\nabla_x^2 u^* - h_{xx}^*), \\ c_{yy}^* &= c_{yy}^* + (\nabla_y^2 u^* - h_{yy}^*), \\ c_{xy}^* &= c_{xy}^* + (\nabla_{xy} u^* - h_{xy}^*). \end{aligned} \tag{34}$$

$(u^*, d_x^*, d_y^*, d_{xy}^*, h_{xx}^*, h_{yy}^*, b_x^*, b_y^*, c_{xy}^*, c_{xx}^*, c_{yy}^*)$ is a fixed point of (27–29), consequently if the modified Split Bregman iteration converges, it converges to a solution of the problem.

Let denote the errors by

$$u_e^k = u^k - u^*, \quad d_{x_e}^k = d_x^k - d_x^*, \quad d_{y_e}^k = d_y^k - d_x^*, \quad b_{x_e}^k = b_x^k - b_x^*,$$
$$b_{y_e}^k = b_y^k - b_y^*, \quad h_{xy_e}^k = h_{xy}^k - h_{xy}^*, \quad h_{xx_e}^k = h_{xx}^k - h_{xx}^*, \quad h_{yy_e}^k = h_{yy}^k - h_{yy}^*,$$
$$c_{xy_e}^k = c_{xy}^k - c_{xy}^*, \quad c_{xx_e}^k = c_{xx}^k - c_{xx}^*, \quad c_{yy_e}^k = c_{yy}^k - c_{yy}^*.$$

From the Euler–Lagrange condition for (27) by subtracting Eq. (32) we obtain

$$\begin{aligned}0 = {} & \mu u_e^{k+1} - \lambda\nabla_x(d_{x_e}^{k+1} - \nabla_x u_e^{k+1} - b_{x_e}^{k+1}) - \lambda\nabla_y(d_{y_e}^{k+1} - \nabla_y u_e^{k+1} - b_{y_e}^{k+1}) \\ & + \lambda\nabla_x^2(h_{xx_e}^{k+1} - \nabla_x^2 u_e^{k+1} - c_{xx_e}^{k+1}) + \lambda\nabla_y^2(h_{yy_e}^{k+1} - \nabla_y^2 u_e^{k+1} - c_{yy_e}^{k+1}) \\ & + \lambda\nabla_{xy}(h_{xy_e}^{k+1} - \nabla_{xy} u_e^{k+1} - c_{xy_e}^{k+1});\end{aligned}$$

Then by taking the inner product of both left hand and right hand sides with respect to u_e^{k+1} we obtain

$$\begin{aligned}0 = {} & \mu\|u_e^{k+1}\|^2 + \lambda\|\nabla_x u_e^{k+1}\| - \lambda\langle\nabla_x d_{x_e}^k, u_e^{k+1}\rangle + \lambda\langle\nabla_x b_{x_e}^k, u_e^{k+1}\rangle \\ & + \lambda\|\nabla_y u_e^{k+1}\|^2 - \lambda\langle\nabla_y d_{y_e}^k, u_e^{k+1}\rangle + \lambda\langle\nabla_y^T b_{y_e}^k, u_e^{k+1}\rangle \\ & - \lambda\|\nabla_x^2 u_e^{k+1}\|^2 + \lambda\langle\nabla_x^2 h_{xx_e}^k, u_e^{k+1}\rangle - \lambda\langle\nabla_x^2 c_{xx_e}^k, u_e^{k+1}\rangle \\ & - \lambda\|\nabla_y^2 u_e^{k+1}\|^2 + \lambda\langle\nabla_y^2 h_{yy_e}^k, u_e^{k+1}\rangle - \lambda\langle\nabla_y^2 c_{yy_e}^k, u_e^{k+1}\rangle \\ & - \lambda\|\nabla_{xy} u_e^{k+1}\|^2 + \lambda\langle\nabla_{xy} h_{xy_e}^k, u_e^{k+1}\rangle - \lambda\langle\nabla_{xy} c_{xy_e}^k, u_e^{k+1}\rangle. \end{aligned} \tag{35}$$

By using the same manipulations to the Euler–Lagrange for (28) an to (33), we have:

$$\begin{aligned}0 &= \langle p_x^{k+1} - p_x^*, d_x^{k+1} - d_x^*\rangle + \lambda\|d_{x_e}^{k+1}\| - \lambda\langle\nabla_x u_e^{k+1}, d_{x_e}^{k+1}\rangle - \lambda\langle b_{x_e}^k, d_{x_e}^{k+1}\rangle, \\ 0 &= \langle p_y^{k+1} - p_y^*, d_y^{k+1} - d_y^*\rangle + \lambda\|d_{y_e}^{k+1}\| - \lambda\langle\nabla_y u_e^{k+1}, d_{y_e}^{k+1}\rangle - \lambda\langle b_{y_e}^k, d_{y_e}^{k+1}\rangle, \\ 0 &= \beta\langle q_{xx}^{k+1} - q_{xx}^*, h_{xx}^{k+1} - h_{xx}^*\rangle + \lambda\|h_{xx_e}^{k+1}\| - \lambda\langle\nabla_x^2 u_e^{k+1}, h_{xx_e}^{k+1}\rangle - \lambda\langle c_{xx_e}^k, h_{xx_e}^{k+1}\rangle, \\ 0 &= \beta\langle q_{yy}^{k+1} - q_{yy}^*, h_{yy}^{k+1} - h_{yy}^*\rangle + \lambda\|h_{yy_e}^{k+1}\| - \lambda\langle\nabla_y^2 u_e^{k+1}, h_{yy_e}^{k+1}\rangle - \lambda\langle c_{yy_e}^k, h_{yy_e}^{k+1}\rangle, \\ 0 &= \lambda\|h_{xy_e}^{k+1}\| - \lambda\langle\nabla_y\nabla_x u_e^{k+1}, h_{xy_e}^{k+1}\rangle - \lambda\langle c_{xy_e}^k, h_{xy_e}^{k+1}\rangle.\end{aligned}$$

By adding Eq. (35) side-by-side with the above equations it follows:

$$\begin{aligned}0 = {} & \mu\|u_e^{k+1}\|^2 + \langle p_x^{k+1} - p_x^*, d_x^{k+1} - d_x^*\rangle + \langle p_y^{k+1} - p_y^*, d_y^{k+1} - d_y^*\rangle \\ & + \beta\langle q_{xx}^{k+1} - q_{xx}^*, h_{xx}^{k+1} - h_{xx}^*\rangle + \beta\langle q_{yy}^{k+1} - q_{yy}^*, h_{yy}^{k+1} - h_{yy}^*\rangle \\ & + \lambda\Big(\|\nabla_x u_e^{k+1}\|^2 + \|\nabla_y u_e^{k+1}\|^2 - \|\nabla_x^2 u_e^{k+1}\|^2 - \|\nabla_y^2 u_e^{k+1}\|^2 \\ & - \|\nabla_{xy} u_e^{k+1}\|^2 + \|d_{x_e}^{k+1}\| + \|d_{y_e}^{k+1}\| + \|h_{xy_e}^{k+1}\| + \|h_{xx_e}^{k+1}\| + \|h_{yy_e}^{k+1}\| \\ & - \langle\nabla_x u_e^{k+1}, d_{x_e}^k + d_{x_e}^{k+1}\rangle + \langle b_{x_e}^k, \nabla_x u_e^{k+1} - d_{x_e}^{k+1}\rangle \\ & - \langle\nabla_y u_e^{k+1}, d_{y_e}^k + d_{y_e}^{k+1}\rangle + \langle b_{y_e}^k, \nabla_y u_e^{k+1} - d_{y_e}^{k+1}\rangle \\ & - \langle\nabla_x^2 u_e^{k+1}, h_{xx_e}^k + h_{xx_e}^{k+1}\rangle + \langle c_{xx_e}^k, \nabla_x^2 u_e^{k+1} - h_{xx_e}^{k+1}\rangle \\ & - \langle\nabla_y^2 u_e^{k+1}, h_{xx_e}^k + h_{yy_e}^{k+1}\rangle + \langle c_{yy_e}^k, \nabla_y^2 u_e^{k+1} - h_{yy_e}^{k+1}\rangle \\ & - \langle\nabla_{xy} u_e^{k+1}, h_{xy_e}^k + h_{xy_e}^{k+1}\rangle + \langle c_{xy_e}^k, \nabla_{xy} u_e^{k+1} - h_{xy_e}^{k+1}\rangle\Big). \end{aligned} \tag{36}$$

By subtracting the first equation of (30) by the first equation of (34) we get:

$$b_{x_e}^{k+1} = b_{x_e}^k + \nabla_x u_e^{k+1} - d_{x_e}^{k+1}.$$

It follows

$$\begin{aligned}\|b_{x_e}^{k+1}\|^2 = {} & \|b_{x_e}^k + \nabla_x u_e^{k+1} - d_{x_e}^{k+1}\|^2 = \|b_{x_e}^k\|^2 + \|\nabla_x u_e^{k+1} - d_{x_e}^{k+1}\|^2 \\ & + 2\langle b_{x_e}^k, \nabla_x u_e^{k+1} - d_{x_e}^{k+1}\rangle.\end{aligned}$$

This leads to

$$\langle b_{x_e}^k, \nabla_x u_e^{k+1} - d_{x_e}^{k+1}\rangle = \frac{1}{2}(\|b_{x_e}^{k+1}\|^2 + \|b_{x_e}^k\|) - \frac{1}{2}\|\nabla_x u_e^{k+1} - d_{x_e}^{k+1}\|^2. \tag{37}$$

Similarly, the same manipulations applied to the remaining equations of (30) and (34) give:

$$\begin{aligned}
\langle b_{y_e}^k, \nabla_y u_e^{k+1} - d_{y_e}^{k+1}\rangle &= \frac{1}{2}(\|b_{y_e}^{k+1}\|^2 - \|b_{y_e}^k\|^2) - \frac{1}{2}\|\nabla_y u_e^{k+1} - d_{y_e}^{k+1}\|^2,\\
\langle c_{xx_e}^k, \nabla_x^2 u_e^{k+1} - h_{xx_e}^{k+1}\rangle &= \frac{1}{2}(\|c_{xx_e}^{k+1}\|^2 - \|c_{xx_e}^k\|^2) - \frac{1}{2}\|\nabla_x^2 u_e^{k+1} - h_{xx_e}^{k+1}\|^2,\\
\langle c_{yy_e}^k, \nabla_y^2 u_e^{k+1} - h_{yy_e}^{k+1}\rangle &= \frac{1}{2}(\|c_{yy_e}^{k+1}\|^2 - \|c_{yy_e}^k\|^2) - \frac{1}{2}\|\nabla_y^2 u_e^{k+1} - h_{yy_e}^{k+1}\|^2,\\
\langle c_{xy_e}^k, \nabla_{xy} u_e^{k+1} - h_{xy_e}^{k+1}\rangle &= \frac{1}{2}(\|c_{xy_e}^{k+1}\|^2 - \|c_{xy_e}^k\|^2) - \frac{1}{2}\|\nabla_{xy} u_e^{k+1} - h_{xy_e}^{k+1}\|^2.
\end{aligned} \tag{38}$$

Then we substitute properly Eqs. (37) and (38) into Eq. (36):

$$\begin{aligned}
&\frac{\lambda}{2}\left(\|b_{x_e}^k\|^2 - \|b_{x_e}^{k+1}\|^2\right) + \frac{\lambda}{2}\left(\|b_{y_e}^k\|^2 - \|b_{y_e}^{k+1}\|^2\right) + \frac{\lambda}{2}\left(\|c_{xx_e}^k\|^2 - \|c_{xx_e}^{k+1}\|^2\right)\\
&+ \frac{\lambda}{2}\left(\|c_{yy_e}^k\|^2 - \|c_{yy_e}^{k+1}\|^2\right) + \frac{\lambda}{2}\left(\|c_{xy_e}^k\|^2 - \|c_{xy_e}^{k+1}\|^2\right)\\
&= \mu\|u_e^{k+1}\|^2 + \langle p_x^{k+1} - p_x^*, d_x^{k+1} - d_x^*\rangle + \langle p_y^{k+1} - p_y^*, d_y^{k+1} - d_y^*\rangle\\
&+ \beta\langle q_{xx}^{k+1} - q_{xx}^*, h_{xx}^{k+1} - h_{xx}^*\rangle + \beta\langle q_{yy}^{k+1} - q_{yy}^*, h_{yy}^{k+1} - h_{yy}^*\rangle\\
&+ \lambda\Big(\|\nabla_x u_e^{k+1}\|^2 + \|\nabla_y u_e^{k+1}\|^2 - \|\nabla_x^2 u_e^{k+1}\|^2 - \|\nabla_y^2 u_e^{k+1}\|^2\\
&- \|\nabla_{xy} u_e^{k+1}\|^2 + \|d_{x_e}^{k+1}\|^2 + \|d_{y_e}^{k+1}\|^2 + \|h_{xy_e}^{k+1}\|^2 + \|h_{xx_e}^{k+1}\|^2 + \|h_{yy_e}^{k+1}\|^2\\
&- \langle \nabla_x u_e^{k+1}, d_{x_e}^k + d_{x_e}^{k+1}\rangle - \frac{1}{2}\|\nabla_x u_e^{k+1} - d_{x_e}^{k+1}\|^2\\
&- \langle \nabla_y u_e^{k+1}, d_{y_e}^k + d_{y_e}^{k+1}\rangle - \frac{1}{2}\|\nabla_y u_e^{k+1} - d_{y_e}^{k+1}\|^2\\
&- \langle \nabla_x^2 u_e^{k+1}, h_{xx_e}^k + h_{xx_e}^{k+1}\rangle - \frac{1}{2}\|\nabla_x^2 u_e^{k+1} - h_{xx_e}^{k+1}\|^2\\
&- \langle \nabla_y^2 u_e^{k+1}, h_{xx_e}^k + h_{yy_e}^{k+1}\rangle - \frac{1}{2}\|\nabla_y^2 u_e^{k+1} - h_{yy_e}^{k+1}\|^2\\
&- \langle \nabla_{xy} u_e^{k+1}, h_{xy_e}^k + h_{xy_e}^{k+1}\rangle - \frac{1}{2}\|\nabla_{xy} u_e^{k+1} - h_{xy_e}^{k+1}\|^2\Big).
\end{aligned} \tag{39}$$

□

After suitable manipulations, applying properly the properties of the norm to the terms involved the right-hand side, the above equation becomes:

$$\begin{aligned}
&\frac{\lambda}{2}\left(\|b_{x_e}^k\|^2 - \|b_{x_e}^{k+1}\|^2\right) + \frac{\lambda}{2}\left(\|b_{y_e}^k\|^2 - \|b_{y_e}^{k+1}\|^2\right) + \frac{\lambda}{2}\left(\|c_{xx_e}^k\|^2 - \|c_{xx_e}^{k+1}\|^2\right)\\
&+ \frac{\lambda}{2}\left(\|c_{yy_e}^k\|^2 - \|c_{yy_e}^{k+1}\|^2\right) + \frac{\lambda}{2}\left(\|c_{xy_e}^k\|^2 - \|c_{xy_e}^{k+1}\|^2\right)\\
&= \mu\|u_e^{k+1}\|^2 + \langle p_x^{k+1} - p_x^*, d_x^{k+1} - d_x^*\rangle + \langle p_y^{k+1} - p_y^*, d_y^{k+1} - d_y^*\rangle\\
&+ \beta\langle q_{xx}^{k+1} - q_{xx}^*, h_{xx}^{k+1} - h_{xx}^*\rangle + \beta\langle q_{yy}^{k+1} - q_{yy}^*, h_{yy}^{k+1} - h_{yy}^*\rangle\\
&+ \lambda\Big(\frac{1}{2}\|\nabla_x u_e^{k+1} - d_{x_e}^k\|^2 + \frac{1}{2}\|d_{x_e}^{k+1}\|^2 - \frac{1}{2}\|d_{x_e}^k\|^2 + \frac{1}{2}\|\nabla_y u_e^{k+1} - d_{y_e}^k\|^2\\
&+ \frac{1}{2}\|d_{y_e}^{k+1}\|^2 - \frac{1}{2}\|d_{y_e}^k\|^2 - 2\|\nabla_x^2 u_e^{k+1}\|^2 + \frac{1}{2}\|\nabla_x^2 u_e^{k+1} - h_{xx_e}^k\|^2\\
&+ \frac{1}{2}\|h_{xx_e}^{k+1}\|^2 - \frac{1}{2}\|h_{xx_e}^k\|^2 - 2\|\nabla_y^2 u_e^{k+1}\|^2 + \frac{1}{2}\|\nabla_y^2 u_e^{k+1} - h_{yy_e}^k\|^2\\
&+ \frac{1}{2}\|h_{yy_e}^{k+1}\|^2 - \frac{1}{2}\|h_{yy_e}^k\|^2 - 2\|\nabla_{xy} u_e^{k+1}\|^2 + \frac{1}{2}\|\nabla_{xy} u_e^{k+1} - h_{xy_e}^k\|^2\\
&+ \frac{1}{2}\|h_{xy_e}^{k+1}\|^2 - \frac{1}{2}\|h_{xy_e}^k\|^2\Big).
\end{aligned} \tag{40}$$

Furthermore, we sum the above equation from $k = 0$ to $k = K$:

$$\begin{aligned}
&\frac{\lambda}{2}\left(\|b_{x_e}^0\|^2 - \|b_{x_e}^{K+1}\|^2\right) + \frac{\lambda}{2}\left(\|b_{y_e}^0\|^2 - \|b_{y_e}^{K+1}\|^2\right) + \frac{\lambda}{2}\left(\|c_{xx_e}^0\|^2 - \|c_{xx_e}^{K+1}\|^2\right)\\
&+ \frac{\lambda}{2}\left(\|c_{yy_e}^0\|^2 - \|c_{yy_e}^{K+1}\|^2\right) + \frac{\lambda}{2}\left(\|c_{xy_e}^0\|^2 - \|c_{xy_e}^{K+1}\|^2\right)
\end{aligned}$$

$$
\begin{aligned}
&= \mu \sum_{k=0}^{K} \|u_e^{k+1}\|^2 + \sum_{k=0}^{K} \langle p_x^{k+1} - p_x^*, d_x^{k+1} - d_x^* \rangle + \sum_{k=0}^{K} \langle p_y^{k+1} - p_y^*, d_y^{k+1} - d_y^* \rangle \\
&+ \beta \sum_{k=0}^{K} \langle q_{xx}^{k+1} - q_{xx}^*, h_{xx}^{k+1} - h_{xx}^* \rangle + \beta \sum_{k=0}^{K} \langle q_{yy}^{k+1} - q_{yy}^*, h_{yy}^{k+1} - h_{yy}^* \rangle \\
&+ \lambda \Big(\frac{1}{2} \sum_{k=0}^{K} \|\nabla_x u_e^{k+1} - d_{x_e}^k\|^2 + \frac{1}{2} \|d_{x_e}^{K+1}\|^2 + \frac{1}{2} \sum_{k=0}^{K} \|\nabla_y u_e^{k+1} - d_{y_e}^k\|^2 \\
&+ \frac{1}{2} \|d_{y_e}^{K+1}\|^2 - 2 \sum_{k=0}^{K} \|\nabla_x^2 u_e^{k+1}\|^2 + \frac{1}{2} \sum_{k=0}^{K} \|\nabla_x^2 u_e^{k+1} - h_{xx_e}^k\|^2 \\
&+ \frac{1}{2} \|h_{xx_e}^{K+1}\|^2 - 2 \sum_{k=0}^{K} \|\nabla_y^2 u_e^{k+1}\|^2 + \frac{1}{2} \sum_{k=0}^{K} \|\nabla_y^2 u_e^{k+1} - h_{yy_e}^k\|^2 \\
&+ \frac{1}{2} \|h_{yy_e}^{K+1}\|^2 - 2 \sum_{k=0}^{K} \|\nabla_y \nabla_x u_e^{k+1}\|^2 + \frac{1}{2} \|\nabla_{xy} u_e^{k+1} - h_{xy_e}^k\|^2 \\
&+ \frac{1}{2} \|h_{xy_e}^{K+1}\|^2 \Big) - \frac{1}{2} \|d_{x_e}^0\|^2 - \frac{1}{2} \|d_{y_e}^0\|^2 - \frac{1}{2} \|h_{xx_e}^0\|^2 - \frac{1}{2} \|h_{yy_e}^0\|^2 - \frac{1}{2} \|h_{xy_e}^0\|^2. \qquad (41)
\end{aligned}
$$

We recall that, for any convex function J, by definition (see [7]) of the Bregman distance associated with J

$$D_J^s(z,t) := J(z) - J(t) - \langle s, z - t \rangle,$$

with $s \in \partial J(t)$, follow the equation:

$$D_J^p(u,v) + D_J^q(v,u) = \langle q - p, u - v \rangle \quad \forall p \in \partial J(u), q \in \partial J(v). \qquad (42)$$

Furthermore, the non-negativity of the Bregman distance implies that

$$\langle q - p, u - v \rangle \geq 0.$$

Since both the functions $\|\cdot\|$ and *log-sum-exp* are convex we have

$$\langle p_x^{k+1} - p_x^*, d_x^{k+1} - d_x^* \rangle \geq 0, \quad \forall k$$

and the same is true for the remaining inner products involved in (41). Therefore all terms in the right-hand member are nonnegative and this leads to the following inequality:

$$
\begin{aligned}
&\frac{\lambda}{2} \|b_{x_e}^0\|^2 + \frac{\lambda}{2} \|b_{y_e}^0\|^2 + \frac{\lambda}{2} \|c_{xx_e}^0\|^2 + \frac{\lambda}{2} \|c_{yy_e}^0\|^2 + \frac{\lambda}{2} \|c_{xy_e}^0\|^2 + + \frac{1}{2} \|d_{x_e}^0\|^2 \\
&+ \frac{1}{2} \|d_{y_e}^0\|^2 + \frac{1}{2} \|h_{xx_e}^0\|^2 + \frac{1}{2} \|h_{yy_e}^0\|^2 + \frac{1}{2} \|h_{xy_e}^0\|^2 + 2\lambda \sum_{k=0}^{K} \|\nabla_x^2 u_e^{k+1}\|^2 \\
&+ 2\lambda \sum_{k=0}^{K} \|\nabla_y^2 u_e^{k+1}\|^2 + 2\lambda \sum_{k=0}^{K} \|\nabla_{xy} u_e^{k+1}\|^2 \\
&\geq \mu \sum_{k=0}^{K} \|u_e^{k+1}\|^2 + \sum_{k=0}^{K} \langle p_x^{k+1} - p_x^*, d_x^{k+1} - d_x^* \rangle + \sum_{k=0}^{K} \langle p_y^{k+1} - p_y^*, d_y^{k+1} - d_y^* \rangle \\
&+ \beta \sum_{k=0}^{K} \langle q_{xx}^{k+1} - q_{xx}^*, h_{xx}^{k+1} - h_{xx}^* \rangle + \beta \sum_{k=0}^{K} \langle q_{yy}^{k+1} - q_{yy}^*, h_{yy}^{k+1} - h_{yy}^* \rangle \\
&+ \lambda \Big(\frac{1}{2} \sum_{k=0}^{K} \|\nabla_x u_e^{k+1} - d_{x_e}^k\|^2 + \frac{1}{2} \|d_{x_e}^{K+1}\|^2 + \frac{1}{2} \sum_{k=0}^{K} \|\nabla_y u_e^{k+1} - d_{y_e}^k\|^2 \\
&+ \frac{1}{2} \sum_{k=0}^{K} \|\nabla_x^2 u_e^{k+1} - h_{xx_e}^k\|^2 + \frac{1}{2} \sum_{k=0}^{K} \|\nabla_y^2 u_e^{k+1} - h_{yy_e}^k\|^2 + \frac{1}{2} \|\nabla_{xy} u_e^{k+1} - h_{xy_e}^k\|^2 \\
&+ \frac{1}{2} \|d_{y_e}^{K+1}\|^2 + \frac{1}{2} \|h_{xx_e}^{K+1}\|^2 + \frac{1}{2} \|h_{yy_e}^{K+1}\|^2 + \frac{1}{2} \|h_{xy_e}^{K+1}\|^2 \Big). \qquad (43)
\end{aligned}
$$

In particular

$$\frac{\lambda}{2}\|b^0_{x_e}\|^2+\frac{\lambda}{2}\|b^0_{y_e}\|^2+\frac{\lambda}{2}\|c^0_{xx_e}\|^2+\frac{\lambda}{2}\|c^0_{yy_e}\|^2+\frac{\lambda}{2}\|c^0_{xy_e}\|^2++\frac{1}{2}\|d^0_{x_e}\|^2 + \frac{1}{2}\|d^0_{y_e}\|^2+\frac{1}{2}\|h^0_{xx_e}\|^2+\frac{1}{2}\|h^0_{yy_e}\|^2+\frac{1}{2}\|h^0_{xy_e}\|^2+2\lambda\sum_{k=0}^{K}\|\nabla^2_x u^{k+1}_e\|^2 + 2\lambda\sum_{k=0}^{K}\|\nabla^2_y u^{k+1}_e\|^2+2\lambda\sum_{k=0}^{K}\|\nabla_y\nabla_x u^{k+1}_e\|^2\geq\mu\sum_{k=0}^{K}\|u^{k+1}_e\|^2. \tag{44}$$

The series $\sum_{k=0}^{+\infty}\|\nabla^2_x u^{k+1}_e\|^2$ converges (since $\|\nabla^2_x u^{k+1}_e\|\leq\delta_1$) and the same holds true for the remaining series involved in the left-hand side). Then we have:

$$\sum_{k=0}^{+\infty}\|u^{k+1}_e\|^2<+\infty,$$

where $u^{k+1}_e=u^{k+1}-u^*$ and therefore:

$$\lim_{k\to+\infty}\|u^{k+1}-u^*\|=0.$$

References

[1] M.V. Afonso, J.M. Bioucas-Dias, M. Figueiredo, Fast image recovery using variable splitting and constrained optimization, IEEE Trans. Image Process. 19 (9) (2010) 2345–2356.
[2] L. Antonelli, V. De Simone, D. di Serafino, On the application of the spectral projected gradient method in image segmentation, J. Math. Imaging Vis. 54 (1) (2016) 106–116.
[3] A. Benfenati, V. Ruggiero, Image regularization for Poisson data, J. Phys.: Conf. Ser. 657 (1) (2015) 1–6.
[4] A. Benfenati, V. Ruggiero, Inexact Bregman iteration for deconvolution of superimposed extended and point sources, Commun. Nonlinear Sci. Numer. Simul. 20 (3) (2015) 882–896.
[5] S. Boyd, N. Parikh, E. Chu, B. Peleato, J. Eckstein, Distributed optimization and statistical learning via the alternating direction method of multipliers, Found. Trends Mach. Learn. 3 (1) (2011) 1–122. http://dx.doi.org/10.1561/2200000016.
[6] S. Boyd, L. Vandenberghe, Convex Optimization, Cambridge University Press, 2004.
[7] L.M. Bregman, A relaxation method of finding a common point of convex sets and its application to the solution of problems in convex programming, Zhurnal Vychislitel'noi Mat. Mat. Fiz. 7 (3) (1967) 620–631.
[8] J.F. Cai, S. Osher, Z. Shen, Split Bregman methods and frame based image restoration., Multiscale Model. Simul. 8 (2) (2009) 337–369. http://dx.doi.org/10.1137/090753504.
[9] R. Campagna, S. Crisci, S. Cuomo, A. Galletti, L. Marcellino, A second order derivative scheme based on Bregman algorithm class, AIP Conf. Proc. 1776 (2016) 040007, doi:10.1063/1.4965319.
[10] A. Chambolle, An algorithm for total variation minimization and applications, J. Math. Imaging Vis. 20 (1–2) (2004) 89–97, doi:10.1023/B:JMIV.0000011325.36760.1e.
[11] A. Chambolle, P.L. Lions, Image recovery via total variation minimization and related problems., Numer. Math. 76 (3) (1997) 167–188, doi:10.1007/s002110050258.
[12] S. Cuomo, P. De Michele, A. Galletti, L. Marcellino, A GPU parallel implementation of the local principal component analysis overcomplete method for DW image denoising, in: Proceedings of IEEE Symposium on Computers and Communication, ISCC 2016, Messina, Italy, June 27–30, 2016, pp. 26–31, doi:10.1109/ISCC.2016.7543709.
[13] S. Cuomo, A. Galletti, L. Marcellino, A GPU algorithm in a distributed computing system for 3d MRI denoising, in: Proceedings of the 10th International Conference on P2P, Parallel, Grid, Cloud and Internet Computing, 3PGCIC 2015, Krakow, Poland, November 4–6, 2015, pp. 557–562, doi:10.1109/3PGCIC.2015.77.
[14] R. De Asmundis, D. di Serafino, G. Landi, On the regularizing behavior of the sda and sdc gradient methods in the solution of linear ill-posed problems, J. Comput. Appl. Math. 302 (2016) 81–93, doi:10.1016/j.cam.2016.01.007.
[15] P. Getreuer, Rudin–Osher–Fatemi total variation denoising using split Bregman, Image Process. On Line 2 (2012) 74–95.
[16] T. Goldstein, X. Bresson, S. Osher, Geometric applications of the split Bregman method: segmentation and surface reconstruction, J. Sci. Comput. 45 (1) (2010) 272–293.
[17] T. Goldstein, S. Osher, The split Bregman method for l1-regularized problems, SIAM J. Imaging Sci. 2 (2) (2009) 323–343, doi:10.1137/080725891.
[18] K. Hammernik, T. Wrfl, T. Pock, A. Maier, A Deep Learning Architecture for Limited-angle Computed Tomography Reconstruction, 2017, 92–97. doi: 10.1007/978-3-662-54345-0_25.
[19] A. Lanza, S. Morigi, F. Sgallari, Convex Image Denoising via Non-convex Regularization with Parameter Selection 56(2) (2016) 195–220. doi: 10.1007/s10851-016-0655-7.
[20] W. Li, Q. Li, W. Gong, S. Tang, Total variation blind deconvolution employing split bregman iteration, J. Vis. Commun. Image Represent. 23 (3) (2012) 409–417.
[21] D. Lustig, M. Martonosi, Reducing GPU offload latency via fine-grained CPU–GPU synchronization, in: Proceedings of the 2013 IEEE 19th International Symposium on High Performance Computer Architecture, HPCA, IEEE, 2013, pp. 354–365.
[22] S. Morigi, L. Reichel, F. Sgallari, Fractional Tikhonov Regularization with a Nonlinear Penalty Term 324 (2017) 142–154. doi: 10.1016/j.cam.2017.04.017.
[23] F. Piccialli, S. Cuomo, P. De Michele, A Regularized MRI Image Reconstruction Based on Hessian Penalty Term on CPU/GPU Systems 18(2013) 2643–2646. doi: 10.1016/j.procs.2013.06.001.
[24] T.M. Quan, S. Han, H. Cho, W.K. Jeong, Multi-GPU reconstruction of dynamic compressed sensing MRI, in: Proceedings of International Conference on Medical Image Computing and Computer-Assisted Intervention, MICCAI, vol. 3, 2015, pp. 484–492.
[25] L.I. Rudin, S. Osher, E. Fatemi, Nonlinear total variation based noise removal algorithms, Physica D 60 (1–4) (1992) 259–268, doi:10.1016/0167-2789(92)90242-F.
[26] S. Setzer, G. Steidl, T. Teuber, Deblurring Poissonian images by split Bregman techniques, J. Vis. Commun. Image Represent. 21 (3) (2010) 193–199.
[27] G. Steidl, A note on the dual treatment of higher-order regularization functionals, Computing 76 (1–2) (2006) 135–148, doi:10.1007/s00607-005-0129-z.

[28] X.C. Tai, C. Wu, Augmented Lagrangian method, dual methods and split Bregman iteration for rof model, Scale Space Var. Methods Comput. Vis. (2009) 502–513. ISBN:978-3-642-02256-2.
[29] M. Zanetti, V. Ruggiero, J. Miranda, Numerical minimization of a second-order functional for image segmentation, Commun. Nonlinear Sci. Numer. Simul. 36 (2016) 528–548, doi:10.1016/j.cnsns.2015.12.018.